

## Article

# Green Synthesis of Antibacterial Silver Nanocolloids with Agroindustrial Waste Extracts, Assisted by LED Light

Ambar Cañadas <sup>1</sup>, Arleth Gualle <sup>1</sup>, Karla Vizuete <sup>2</sup>, Alexis Debut <sup>2</sup>, Patricio Rojas-Silva <sup>3</sup>,  
Sebastian Ponce <sup>1,\*</sup> and Lourdes M. Orejuela-Escobar <sup>1,4,5,\*</sup>

<sup>1</sup> Department of Chemical Engineering, Universidad San Francisco de Quito USFQ, Diego de Robles s/n y Av. Interoceánica, Quito 170157, Ecuador

<sup>2</sup> Centro de Nanociencia y Nanotecnología, Universidad de las Fuerzas Armadas ESPE, Sangolquí 171103, Ecuador

<sup>3</sup> Instituto de Microbiología, Universidad San Francisco de Quito USFQ, Diego de Robles s/n y Av. Interoceánica, Quito 170157, Ecuador

<sup>4</sup> Instituto de Investigaciones Biológicas y Ambientales BIOSFERA, Universidad San Francisco de Quito USFQ, Diego de Robles s/n y Av. Interoceánica, Quito 170157, Ecuador

<sup>5</sup> Instituto de Investigaciones en Biomedicina, Universidad San Francisco de Quito USFQ, Diego de Robles s/n y Av. Interoceánica, Quito 170157, Ecuador

\* Correspondence: sponce@usfq.edu.ec (S.P.); lorejuela@usfq.edu.ec (L.M.O.-E.)



**Citation:** Cañadas, A.; Gualle, A.; Vizuete, K.; Debut, A.; Rojas-Silva, P.; Ponce, S.; Orejuela-Escobar, L.M. Green Synthesis of Antibacterial Silver Nanocolloids with Agroindustrial Waste Extracts, Assisted by LED Light. *Colloids Interfaces* **2022**, *6*, 74.

<https://doi.org/10.3390/colloids6040074>

Academic Editors: Aleksandra Szcześ, Wuge Briscoe and Reinhard Miller

Received: 1 September 2022

Accepted: 25 November 2022

Published: 1 December 2022

**Publisher's Note:** MDPI stays neutral with regard to jurisdictional claims in published maps and institutional affiliations.



**Copyright:** © 2022 by the authors. Licensee MDPI, Basel, Switzerland. This article is an open access article distributed under the terms and conditions of the Creative Commons Attribution (CC BY) license (<https://creativecommons.org/licenses/by/4.0/>).

**Abstract:** Herein, the green synthesis of silver nanoparticles (AgNPs), assisted by LED light, using the aqueous extracts of agroindustrial waste products, such as avocado seeds (ASs), cocoa pod husks (CPHs), and orange peels (OPs), is presented. Surface plasmon resonance analysis showed faster and complete NP formation when irradiated with blue LED light. Green and red light irradiation showed non- and limited nanoparticle formation. TEM analyses confirmed the semispherical morphology of the synthesized AgNPs, with the exception of OP–AgNPs, which showed agglomeration during the light irradiation. For AS–AgNPs and CPH–AgNPs, the average particle diameter was about 15 nm. Interestingly, the CPH extract demonstrated faster nanoparticle formation as compared to the AS extract (100 min vs. 250 min irradiation time, respectively). FTIR spectroscopy assessed the involvement of diverse functional groups of the bioactive phytochemicals present in the plant extracts during nanoparticle photobiosynthesis. The antioxidant activity, as determined by ferric reducing antioxidant power (FRAP) assay, varied from 1323.72  $\mu\text{mol TE/mL}$  in the AS aqueous extract to 836.50  $\mu\text{mol TE/mL}$  in the CPH aqueous extract. The total polyphenol content was determined according to the Folin–Ciocalteu procedure; the AS aqueous extract exhibited a higher polyphenol content (1.54 mg GAE/g) than did the CPH aqueous extract (0.948 mg GAE/g). In vitro antibacterial assays revealed that the AS–AgNPs exhibited promising antibacterial properties against pathogenic bacteria (*E. Coli*), whereas the CPH–AgNPs showed antibacterial activity against *S. aureus* and *E. coli*. The green synthesis of AgNPs using AS, CPH, and OP aqueous extracts reported in this work is environmentally friendly and cost-effective, and it paves the way for future studies related to agroindustrial waste valorization for the production of advanced nanomaterials, such as antibacterial AgNPs, for potential biomedical, industrial, and environmental applications.

**Keywords:** green synthesis; agroindustrial waste extracts; bioactive phytochemicals; antibacterial activity; nanoparticles; circular bioeconomy

## 1. Introduction

The world's population growth and the concern for healthy diets have increased the awareness of the nutritional value of fruits and vegetables. Thus, their growing consumption is forcing an expansion of production and supply, which also generates a great volume of agroindustrial waste [1]. These agroindustrial residues and byproducts are not part of the value chain and may have a negative environmental impact. However, despite the

fact that they are secondary raw materials, they are a renewable resource with valuable phytochemicals, such as essential oils, polyphenols, and tannins, among others [2]. Most of these compounds are bioactive, can be recovered from the biomass matrix, and can be used as antioxidant or antimicrobial agents. Ecuador is an agroindustrial country where several tropical crops are traditionally cultivated and exported worldwide, cacao beans and bananas being the main export goods [3]. The worldwide consumption of crops such as avocado and citrus fruits is growing; therefore, the production and export of these crops in Ecuador is also increasing [4–6]. These industries generate residues of around 2,200,000 tons; these residues are currently underutilized, and they pose a waste problem in Ecuador [7]. However, by applying zero waste technologies and biorefining approaches, the value of such waste will increase, thus favoring the circular bioeconomy in Ecuador [2,8].

A variety of metal nanoparticles (MNPs) have been produced through physical and chemical methods, such as laser ablation, evaporation–condensation, ball milling, and chemical reduction, among others. These techniques are normally expensive, toxic, and have a negative environmental impact. Conversely, green synthesis, which uses biological agents such as microorganisms and plants (including medicinal plants) for synthesizing MNPs is an environmentally friendly, affordable, and less-toxic method [9–11]. Among the MNPs, silver nanoparticles (AgNPs) obtained through green synthesis have gained attention since they have antibacterial and antiviral properties, making them the perfect nanomaterial to be used in drug-delivery systems, biomedical device coatings, nanocomposites, and biofilms [12,13]. However, chemically synthesized AgNPs might have cytotoxic and genotoxic effects, triggering oxidative cell and DNA damage, as well as the inhibition of cell proliferation, due to the nature of the reducing agent and capping material used [14]. Therefore, the green synthesis of AgNPs is a sustainable solution.

Extracts made from agroindustrial residues, including avocado seeds, cocoa pod husks, and orange peels, have been reported in literature as reducing and capping agents for NP synthesis, showing enhanced antibacterial properties [15–17]. Moreover, light-induced NP synthesis is an alternative when using plant extracts due to the photochemical properties of their constituents for promoting the reduction of  $\text{Ag}^+$  to  $\text{Ag}^0$  nanospheres [18–20]. In this work, the reducing potential of antioxidant and antibacterial avocado seed (AS), cocoa pod husk (CPH) and orange peel (OP) aqueous extracts, were evaluated for the synthesis of AgNPs assisted by different LED lights—without the addition of any external reducing or capping agent. The antibacterial properties of synthesized nanoparticles were also analyzed.

## 2. Materials and Methods

### 2.1. Materials

Silver nitrate salt ( $\text{AgNO}_3$ ) (reagent grade, Scharlau) and distilled water were used for the synthesis of the silver nanoparticles. The avocado (*Persea americana*) seeds and orange (*Citrus sinensis*) peels used for this research were obtained from local markets and restaurants in the city of Quito. The cocoa (*Theobroma cacao*) pod husks were obtained from the city of Guayaquil and nearby locations.

### 2.2. Extract Preparation and Soxhlet Extraction

Raw material preparation was performed following a standardized method developed in our lab. The avocado seeds (ASs) were dried and ground to obtain a particle size between 2 mm and 500  $\mu\text{m}$ , and then they were refrigerated to prevent oxidation. The cocoa pod husks (CPHs) and orange peels (OPs) were first dried at 40 °C for 48 h, and then they were ground. For Soxhlet extraction, 9 g of the raw material was transferred to a thimble, which in turn was placed in an extractor reservoir. A measured amount of 150 mL of distilled water was added to the distillation flask for initiating the extraction process, which was performed in triplicate, over 4 h. The aqueous extract was left to rest until it reached the ambient temperature, approximately 1 h. All of the obtained extracts were concentrated in a rotary evaporator and then lyophilized.

### 2.3. Synthesis of AgNPs, Assisted by Light

The aqueous extracts of the agroindustrial waste (0.01 g mL<sup>-1</sup>) and the AgNO<sub>3</sub> aqueous solution (2.5 mM) were prepared and mixed under dark conditions. For the synthesis of the silver colloids, a mixture of silver nitrate:extract (2:1) was prepared under dark conditions. Then, the solution was illuminated for different lengths of time with a commercial LED floodlight (100 W, IP66) with differing wavelengths (450–660 nm) at room temperature. Aliquots of 300 µL were taken, mixed with 2000 µL of distilled water, and characterized in the UV–Vis spectrophotometer for different periods of time, around 6 h.

### 2.4. Analytical Methods

The absorption spectra of the Ag colloids were recorded using a UV–Vis spectrophotometer (CE 204, CECIL, Buck Scientific, Norwalk, CT, USA) from 300 to 1000 nm. FTIR spectra were recorded in regimes between 650 and 4000 cm<sup>-1</sup> using an Agilent Cary 630, (Agilent Technologies, Santa Clara, CA, USA). The dynamic light scattering (DLS) technique was used for analyzing the hydrodynamic particle size and distribution of the particles using Horiba—LB-550 (Horiba, Kyoto, Japan) equipment. For the study of the size and morphology of the synthesized particles, an FEI Spirit Twin (FEI Company, Hillsboro, OR, USA) transmission electron microscope (TEM) with a LaB6 filament was used, operating at a voltage of 80 kV.

### 2.5. Determination of Antioxidant Activity by Ferric Reducing Antioxidant Power (FRAP) Assay

The FRAP solution was prepared with the following reagents: 300 mM sodium acetate trihydrate buffer pH 3.6; TPTZ (2,4,6-tri-2-pyridinyl-1,3,5-triazine) 10 mM in 40 mM HCl; and 20 mM FeCl<sub>3</sub> hexahydrate. The working FRAP reagent was mixed in a 10:1:1 ratio prior to running the assays. The standard solution was 5 mM Trolox dissolved in ethanol. The different Trolox dilutions were prepared as follows: 500 µM, 400 µM, 250 µM, 200 µM, 100 µM, 75 µM, and 50 µM. For the tests, 900 µL of FRAP reagent and 100 µL of the standard were placed, or the samples were mixed for 15 s and measured at an absorbance of 593 nm. For the blank, the same process was followed, using 900 µL of the FRAP reagent and 100 µL distilled water.

### 2.6. Determination of Total Polyphenols

For the determination of the polyphenols, 0.02 N Folin–Ciocalteu reagent and 75 g/L sodium carbonate were used. Gallic acid (6 mM) was used as the standard for the curve, and different concentrations were prepared, from 3 mM to 0.1875 mM. Then, 100 µL of a sample or the standard solution with 500 µL Folin–Ciocalteu reagent were added, and the mixture was incubated for 5 min at room temperature. A quantity of 400 µL calcium carbonate solution was added, and then it was stored in the dark for 2 h at room temperature. The blank was prepared with 100 µL distilled water and 500 µL Folin–Ciocalteu reagent were added. Then, the same process (as described above) was repeated. Samples were measured at an absorbance of 760 nm; total polyphenols were expressed as mg/g gallic acid equivalents (GAE).

### 2.7. Evaluation of Antibacterial Activity In Vitro

The disc diffusion method was used for the determination of antibacterial activity. The AgNP solutions of the agricultural residue extracts were impregnated in sterile filter paper discs (Whatman Grade 1, size: 6 mm in diameter), dried at 40 °C for 30 min.

For the analyses, we used different types of bacteria: *S. aureus* ATCC 25923, *Escherichia coli* ATCC 25922, and *Pseudomonas aeruginosa* ATCC 27853. Bacteria were cultivated in nutrient agar medium for 48 h at 34 °C, and then, 2–3 colonies were selected and transferred to a saline solution to generate a 0.5 McFarland concentration. With the help of a sterile swab, the bacterial solution was inoculated over the entire surface of the Mueller–Hinton medium agar. The discs impregnated with AgNPs were placed on the surface of the agar and incubated at 34 °C for 24 h.

As a negative control, distilled water was placed on a filter disc. Discs with gentamicin antibiotic concentrations were used as positive controls, and additional discs containing plant residue extracts without nanoparticles were used. The antibacterial activity was determined after 24 h via the diameter of the zone of inhibition, measured in millimeters. The assay was performed in triplicate.

### 3. Results and Discussion

#### 3.1. Nanoparticle Synthesis

Figure 1a shows a schematic representation of the procedure we followed for the NP synthesis using extracts from agroindustrial waste in this study. In summary, LED light irradiation photoactivates the phytochemicals present in the extracts, promoting the reduction process of the silver salt ( $\text{Ag}^+$ ) to  $\text{Ag}^0$  seeds, which subsequently agglomerate, forming AgNPs that are controlled by the remaining biological molecules attached to their surfaces. Particularly, Figure 1b shows an optical photograph of the extract/ $\text{AgNO}_3$  aqueous solution, before and after 6 h of blue LED (450 nm) light irradiation at room temperature. For all mixtures, the solution changed from a yellowish to a dark brown color after light illumination, which indicated the formation of AgNPs. Similar NP formation has been observed using fruit extracts, as reported in previous studies [21]. For control of the light effect, the SPR spectra of nonirradiated samples were recorded. As observed in Figure 1c, no NP formation (dashed line) was noticeable for the same time scale ( $\approx 6$  h).

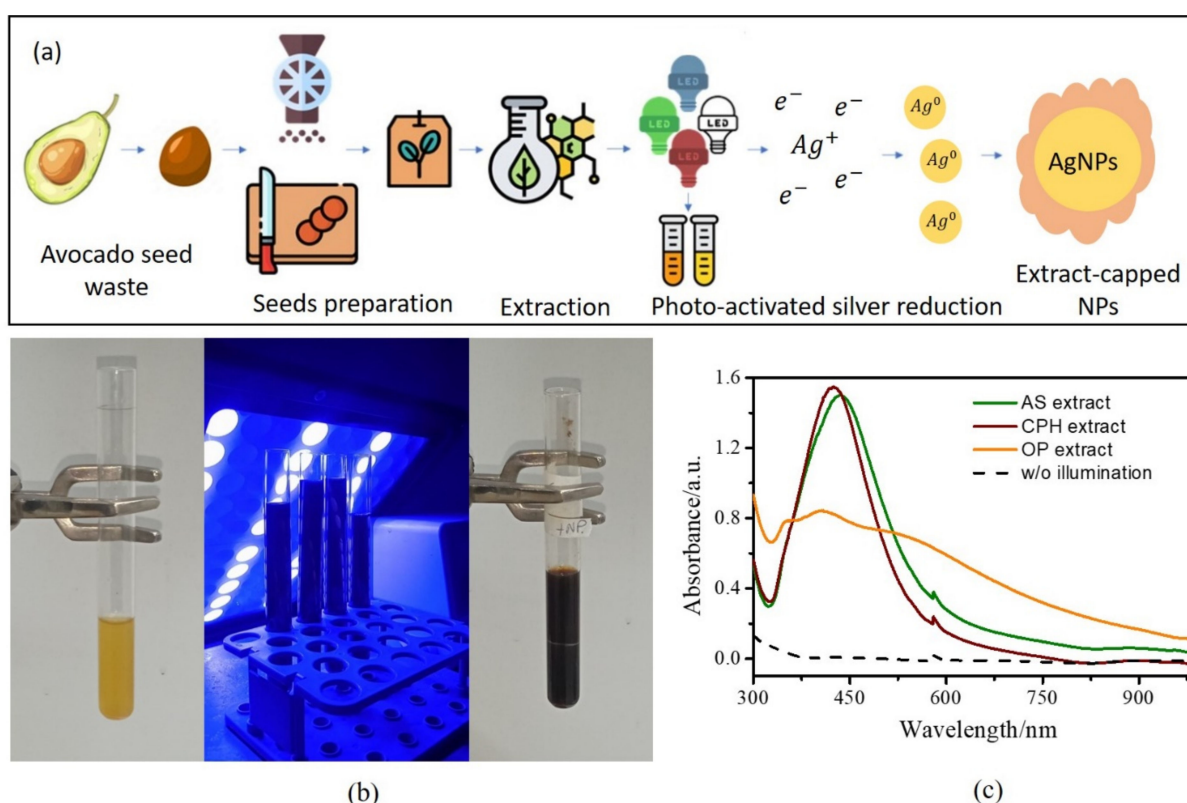


**Figure 1.** (a) Schematic representation of the NP synthesis followed in this work; (b) exemplary image of silver colloid synthesis via blue LED light irradiation; and (c) surface plasmon resonance of colloids synthesized using avocado seed, cocoa pod husk, and orange peel extracts, and a nonirradiated sample, after 6 h blue LED light irradiation.

For the AS and CPH extracts, the formation of characteristic surface plasmon resonance (SPR) for quasi-spherical AgNPs is shown in Figure 1b. In contrast, a broad spectrum for the OP extracts was observed, which indicates the possible formation of big agglomerates

during the NP formation. Therefore, further investigation was only focused on the AS and CPH extracts. The dashed line confirms the lack of NP formation in the dark-storage samples.

To further understand the NPs' formation, SPR spectra of samples using the AS extract, irradiated for different amounts of time, were recorded. An example is shown in Figure 2a. The NP formation started directly after the light irradiation began, with the SPR formation, which rose in intensity until all of the silver salt was consumed. Synthesized colloids were stable during long-term dark-storage. They did not show considerable aggregation and remained stable for up to 1.5 months (see inset, Figure 2a). From this experiment, peak maxima vs. time curves were developed, and the existence of exponential growth was clearly observed until the silver salt had been consumed (see Figure 2b).

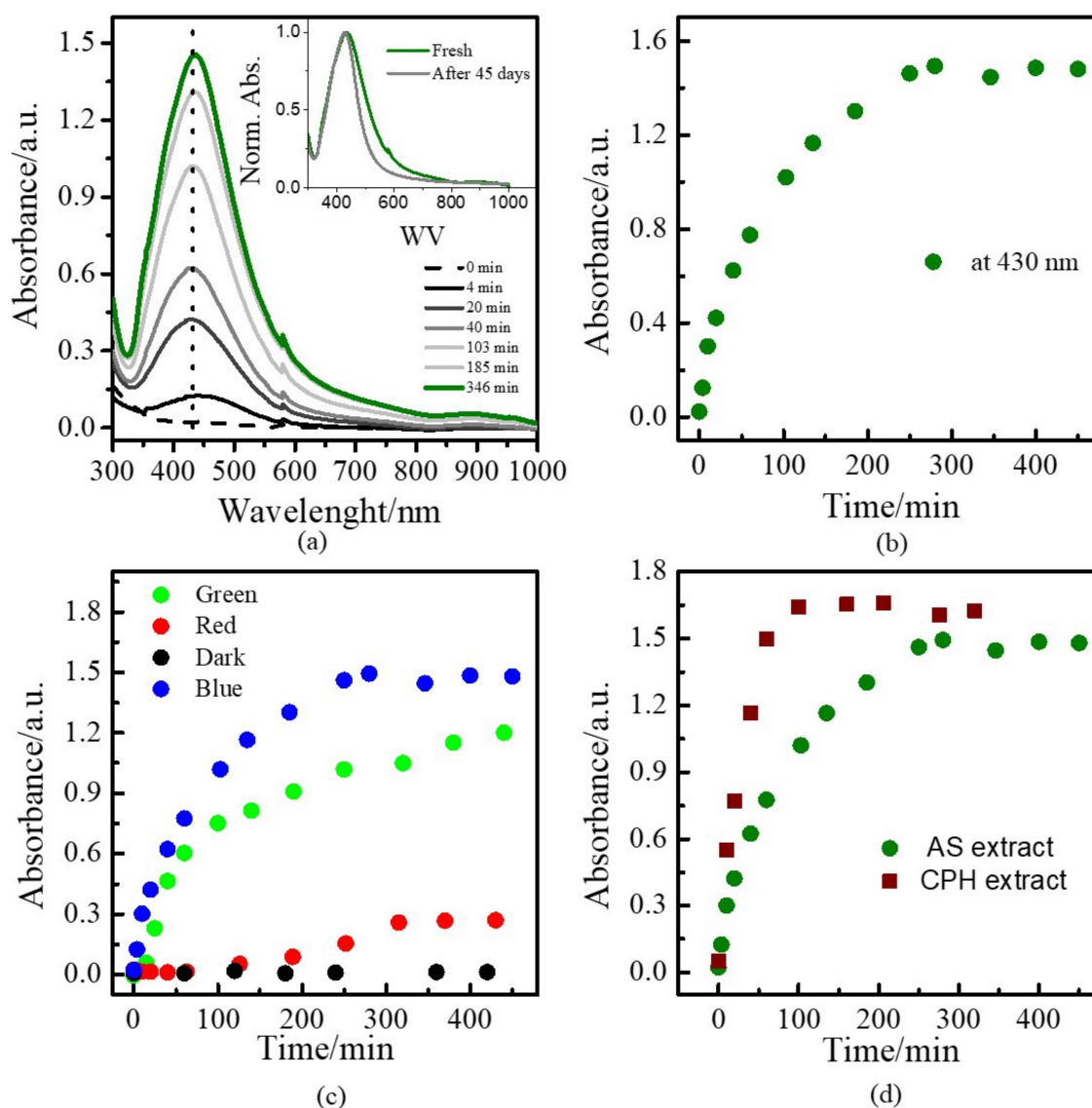


**Figure 2.** UV-vis spectra of blue-light-irradiated samples at different times (a); absorbance at peak maxima vs. time curves of mixture illuminated with blue LED light (inset: normalized absorbance vs. wavelength for a fresh sample and for 45-day-old, dark-storage NPs) (b); with different LED lights (c); and comparison of AS and CPH extracts irradiated with blue light (d), ((a–c): AS extract).

When samples were irradiated with lower-energy wavelengths, limited or no NP formation was observed (see Figure 2c). For green LED light illumination ( $\approx 490$  nm), slow

formation of AgNPs was shown. After 6 h of illumination, the silver salt was not totally consumed (about 20% of the salt remained). In contrast to the blue light irradiation, after 50 min, NP formation was limited to a linear growth pattern. No NP formation was observed for red light irradiation ( $\approx 650$  nm), showing that illumination was not enough for starting NP formation, similar to the nonirradiated samples. After just 250 min, a scarce presence of NP formation was observed. These results show that plant residue-based extracts possibly have biomolecules with chromophore groups that favor the absorption of light under 450 nm for reducing  $\text{Ag}^+$  into  $\text{Ag}^0$ . The irradiation with a lower energy induced NP formation, but at a slower rate, such that the NP agglomeration lasted for a longer time. Therefore, if a sample is irradiated with sunlight, for instance, just the high energy portion of it would be useful for photocatalyzing the reduction process in the green synthesis. Finally, a comparison between the AS and CPH aqueous extracts is shown in Figure 2d. Under blue LED light irradiation, the CPH extracts had a faster reducing effect for NP formation, with complete cluster formation after just 3 h. The CPH and AS extracts showed the same behavior under green and red irradiation. (See Figure S1 in the Supplementary Materials.)

Regarding the size and morphology of the AgNPs, TEM and DLS (see Figure S2 in the Supplementary Materials), characterizations of the blue-LED-light-synthesized AgNPs were performed. TEM images of the AS–AgNP and CPH–AgNP samples showed a quasi-spherical shape with an average diameter of about  $15 \pm 9$  and  $14.8 \pm 8$  nm, respectively (see Figure 3a,b). Moreover, DLS studies showed an average hydrodynamic size of 79 and 66 nm in solution, respectively, which differed with the result obtained via TEM image analysis. This could be related to the presence of unreacted extract around the AgNPs and the screening of bigger particles over smaller ones [22]. It also shows the polydisperse nature of the synthesized NPs. In the case of the AS extracts, the synthesized nanoparticles showed a narrower SPR spectrum and a smaller average nanoparticle size than those reported by previous studies performed without the use of reagents, such as ammonium hydroxide [17].

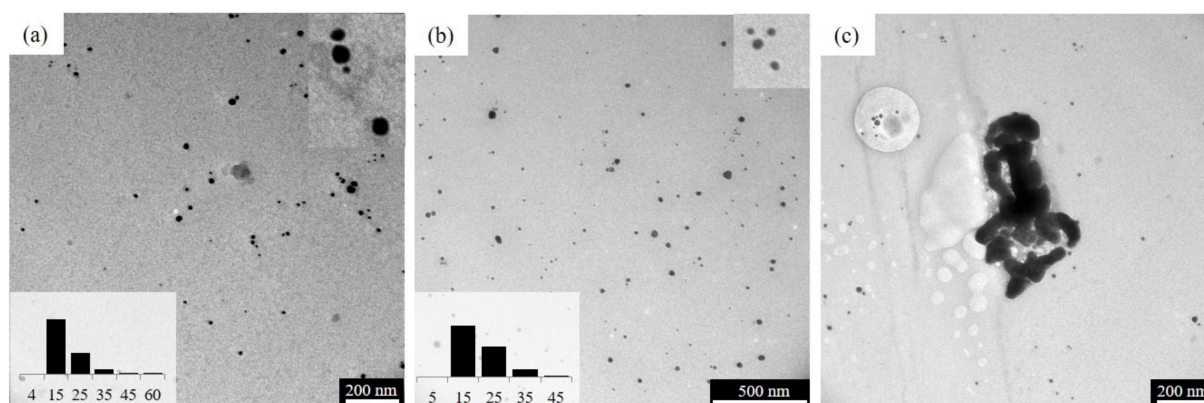


**Figure 3.** TEM image of AgNPs synthesized by blue light irradiation using different agroindustrial waste extracts: (a) avocado seeds, (b) cocoa pod husks, and (c) orange peels.

As expected from the SPR of the AgNPs created with the OP samples, bigger aggregates were present, which was confirmed by TEM (see Figure 3c) and DLS studies, with an average hydrodynamic size of 3070 nm in solution.

It is well-known that water-soluble biomolecules and sugars present in plants act as reducers and capping agents for nanoparticle synthesis. In this study, FTIR spectra were recorded to elucidate the functional groups in the biomolecules that are involved in nanoparticle synthesis. FTIR analyses were conducted on the AS and CPH aqueous extracts (see Figure 4 and Figure S3 in the Supplementary Materials). An example is shown in Figure 4: peaks near  $3250$ ,  $2940$ , and  $1600$   $\text{cm}^{-1}$  are related to O-H, C-H, and

C=O stretch vibrations corresponding to flavonoid/phenolic groups [23,24]. Moreover, stretching vibrations at  $1390\text{ cm}^{-1}$  (C-N) could be associated with the presence of amino groups. The band at  $1013\text{ cm}^{-1}$  might correspond to the C-O and C-N stretching present in aliphatic amines and phenolic compounds [25]. Moreover, FTIR spectra were also recorded for the synthesized NPs using blue LED light. Both evidenced similar spectra, which would indicate the presence of biomolecules at the NPs' surface, which controlled the NPs' agglomeration. This behavior has been also observed in previous studies, where it was attributed to green synthesis using plant extracts [26]. Deeper studies in the identification of the biomolecules involved in the reduction process are required, and our research group is already working on this fascinating topic.

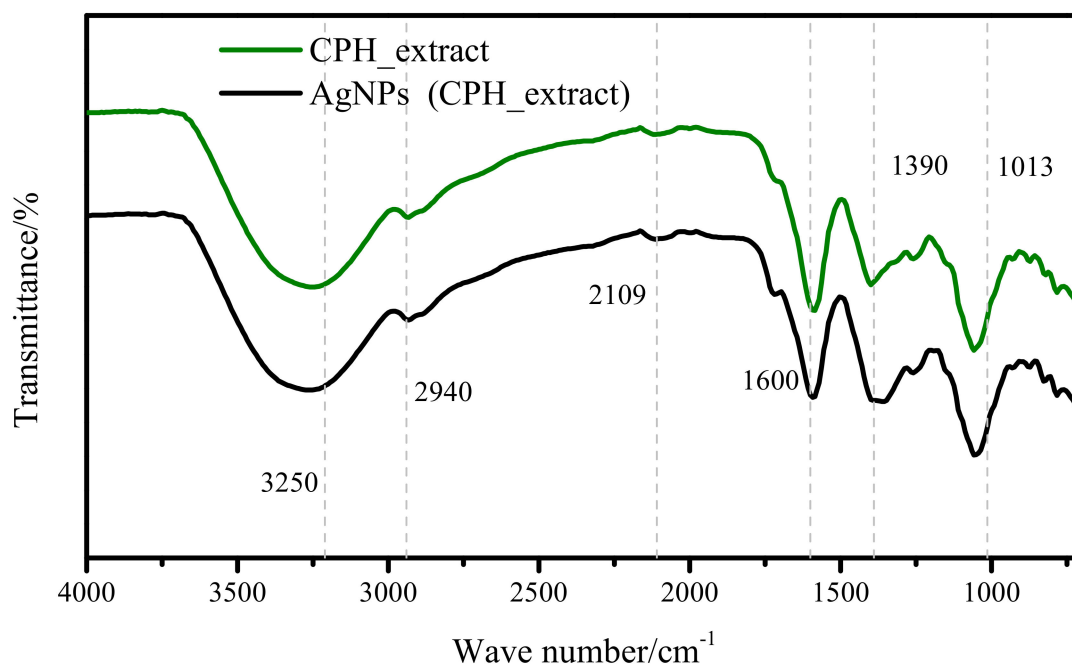


**Figure 4.** FTIR spectra of avocado seed extract and AgNPs synthesized via blue light irradiation.

### 3.2. Determination of Antioxidant Activity and Polyphenol Content of Extracts from Agroindustrial Residues

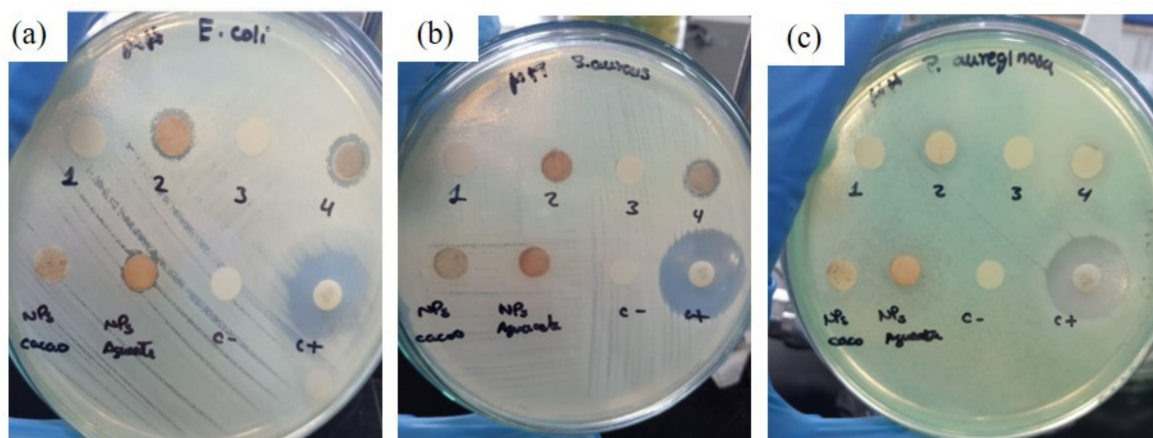
The antioxidant activity was measured using the FRAP method, with a concentration of aqueous extract of  $10\text{ mg/mL}$ . The avocado seed aqueous extract ( $1323.72 \pm 16.78\text{ }\mu\text{mol Trolox equivalents/mL extract}$ ) showed a more significant level of antioxidant activity than did the cocoa pod husk aqueous extract. Therefore, the avocado seed aqueous extract presents a greater potential for reducing the ferric ion ( $\text{Fe}^{3+}$ ) to a ferrous ion ( $\text{Fe}^{2+}$ ), which formed a blue colorimetric complex between  $\text{Fe}^{2+}$  and TPTZ (Table 1). The ability of the avocado seed aqueous extract to eliminate free radicals may be due to the presence of compounds such as tannins, flavonoids, and other polyphenol compounds that act as natural antioxidants [27]. These data correlate with the concentration of polyphenols obtained via the Folin–Ciocalteu method. The results show that the avocado seed aqueous extract ( $1.54 \pm 0.088$ ) contained 1.6 times more polyphenols than the cocoa pod husks ( $0.948 \pm 0.059$ ) per milligram of gallic acid equivalent (GAE) per gram of dry extract. Avocado seed is a residue rich in tannin polyphenols, phenolic acids, and flavonoids, which are the most representative groups, and other polyphenols, such as: (+)-catechin, (–)-epicatechin, and 3-leucoanthocyanidins, which have demonstrated anti-inflammatory properties [28]. Cocoa pod husks contain polyphenols and phenolic acids, such as protocatechuic acid, p-hydroxybenzoic acid, and salicylic acid—flavonols and flavonoid compounds that allow them to be used as potential food preservatives and antioxidants [29].

**Table 1.** Antioxidant activity and polyphenol concentration of aqueous extracts of avocado seeds and cocoa pod husks.

Sample	Antioxidant Activity	Concentration of Total Polyphenols
Aqueous extracts (10 mg/mL)	$\mu\text{mol Trolox equivalents/mL extract}$	$\text{mg GAE/g extract}$
Avocado seeds	$1323.72 \pm 16.78$	$1.54 \pm 0.088$
Cocoa pod husks	$836.50 \pm 14.46$	$0.948 \pm 0.059$

### 3.3. Antibacterial Activity

The AS and CPH aqueous extracts did not show any potential for inhibiting the growth of any of the bacteria used in this investigation. In contrast, AgNPs prepared from extracts of agroindustrial residues exhibited variable antibacterial activity, as shown in Figure 5 and by the values listed in Table 2. The CPH–AgNPs had a higher level of antibacterial potential against pathogens, such as *S. aureus* ( $11.51 \pm 0.035$  mm) and *E. coli* ( $13.48 \pm 0.025$  mm). In the case of the AS–AgNPs, antibacterial activity was only identified in *E. coli*, with a zone of inhibition of  $10.51 \pm 0.097$  mm. Thus, these NPs did not show any effect on the growth of *P. aeruginosa*.

**Figure 5.** Inhibitory effect on different bacteria using silver nanoparticles with extracts of agricultural residues: (1) AS extract, (2) AS–AgNPs, (3) CPH extract, (4) CPH–AgNPs, (C–) Distilled water, (C+) Gentamicin 10  $\mu\text{g}$ , (a) *E. coli*, (b) *S. aureus*, and (c) *P. aeruginosa*.**Table 2.** Antibacterial activity of aqueous extracts and silver nanoparticles from agroindustrial residue extracts against bacterial microorganisms.

Sample	<i>Staphylococcus aureus</i> Inhibition Zone mm (SD)	<i>Escherichia coli</i> Inhibition Zone mm (SD)	<i>Pseudomonas aeruginosa</i> Inhibition Zone mm (SD)
1 AS extract	0.0	0.0	0.0
2 AS-NPs	0.0	$10.51 \pm 0.097$	0.0
3 CPH extract	0.0	0.0	0.0
4 CPH-NPs	$11.51 \pm 0.097$	$13.48 \pm 0.025$	0.0
Negative control Distilled water	0.0	0.0	0.0
Positive control Gentamicin Discs 10 $\mu\text{g}$	$21.10 \pm 0.015$	$17.48 \pm 0.029$	$24.50 \pm 0.045$

AgNPs inhibit the growth of bacteria due to their ability to bind to the cell membrane and modify its permeability, thus triggering the death of a bacterium [23]. This action is

based on the release of silver ions from the NPs, which destroy the cell wall by interacting with sulfur-containing proteins. Also noteworthy is that the plant extracts used as organic matrices for the green synthesis of the AgNPs contain compounds such as tannins, phenols, and flavonoids that could increase antibacterial activity, therefore enhancing the AgNPs' efficacy by interacting with bacteria and inhibiting their development [30]. The variability of the antibacterial activity depends on different factors, such as the concentration of the AgNPs, the type of plant used for the preparation of the extract, and the difference in the cell-wall structure of Gram-positive and Gram-negative bacteria [31].

The AgNPs, when suspended in an extract of agroindustrial residues, have good stability and dispersion, which could contribute to the good interaction with bacteria within the culture medium, as seen in our *in vitro* tests. Additionally, a report by Lateef et al., (2016) demonstrated the antibacterial activity of CPH–AgNPs against multiresistant *K. pneumoniae* and *E. coli*. The results showed zones of inhibition of 10–14 mm with a CPH–AgNP concentration of 40–100 µg/mL. Similar results with *E. coli* were obtained by another research group [32]. This study shows that CPH–AgNPs inhibited the growth of *E. coli* as well as *S. aureus* bacteria with similar results

#### 4. Conclusions

This research demonstrates the ability of aqueous extracts from Ecuadorian agroindustrial residues, such as avocado seeds and cocoa pod husks, to be considered as cost-effective and ecofriendly renewable resources in the green synthesis of AgNPs, assisted by different LED lights, without the addition of any external reducing or capping agent.

Based on surface plasmon spectral analysis, blue LED light was found to be the most effective light for well-defined, quasi-spherical NP formation in the case of both avocado seed and cocoa pod husk extracts. Orange peel extracts were found to not be as effective as the above-mentioned extracts for NP formation under light irradiation. Moreover, from TEM analysis, remarkably, small and well-distributed particles ( $\approx 15$  nm) were obtained using AS and CPH extracts, as compared to the findings of previous works. The results from the FRAP and Folin–Ciocalteu analyses show that the avocado seed aqueous extract had a higher level of antioxidant activity and total polyphenol content compared to the results obtained from the cocoa pod husk extract. These extracts could potentially be used as sources of antioxidants; it is necessary to carry out more in-depth studies to characterize which bioactive compounds are responsible for the antibacterial and antioxidant activity.

Finally, the CPH–AgNPs showed a higher antibacterial potential against pathogens, such as *S. aureus* and *E. coli*. In the case of the AS–AgNPs, antibacterial activity was identified only for *E. coli*. None of the synthesized NPs showed an effect on the growth of *P. aeruginosa*.

All in all, NPs produced via green synthesis mediated by aqueous extracts from agroindustrial residues and byproducts display good properties and may have an impact on biomedical applications, especially in therapeutic healthcare practices, drug-delivery systems, diagnosis platforms, antimicrobial biofilms and coatings for medical devices, as well as in the packing and packaging industries. Therefore, it is important to investigate other agroindustrial residue extracts as media for green synthesis, as well as to determine their other bioactive properties, such as anti-inflammatory, antifungal, antiviral, and larvicidal activity, so as to find novel and effective antimicrobial agents.

**Supplementary Materials:** The following supporting information can be downloaded at: <https://www.mdpi.com/article/10.3390/colloids6040074/s1>, Figure S1: (a) UV-vis spectra of blue light irradiated samples at different times, (b) Absorbance at peak maxima versus time curves of mixture illuminated with different LED lights. (a and b: CPH extract); Figure S2: Particle size distribution curves of synthesized nanoparticles by DLS experimentation (a) AS, (b) CPH, and (c) OP extracts; Figure S3: FTIR spectra of cocoa pod and AgNPs synthesized by blue light irradiation.

**Author Contributions:** Investigation, A.C. and A.G.; lab experimentation, A.C. and A.G.; methodology, A.C.; nanoparticle synthesis, A.C.; characterization, A.C.; extractions, A.G.; determination of antioxidant activity, A.G.; total polyphenol and antibacterial tests, A.G.; material characterization, K.V. and A.D.; data curation, K.V. and A.D.; review and editing, K.V. and A.D.; supply of bacteria and antibacterial test supervision, P.R.-S.; funding, S.P. and L.M.O.-E.; project administration, S.P. and L.M.O.-E.; writing—original draft preparation, S.P. and L.M.O.-E.; supervision, S.P. and L.M.O.-E. All authors have read and agreed to the published version of the manuscript.

**Funding:** This research has been supported by the Poli Grant Program at the Universidad San Francisco de Quito.

**Acknowledgments:** This study has benefitted from the support of the Chemical Engineering Department; the instructors who run the lab equipment; the Agronomy Department, especially Antonio León and Noelia Barriga; and the students and colleagues of our research group, Applied Circular Engineering and Simulation.

**Conflicts of Interest:** The authors declare no conflict of interest.

## References

1. Girotto, F.; Alibardi, L.; Cossu, R. Food waste generation and industrial uses: A review. *Waste Manag.* **2015**, *45*, 32–41. [[CrossRef](#)] [[PubMed](#)]
2. Orejuela-Escobar, L.M.; Landázuri, A.C.; Goodell, B. Second generation biorefining in Ecuador: Circular bioeconomy, zero waste technology, environment and sustainable development: The nexus. *J. Bioresour. Bioprod.* **2021**, *6*, 83–107. [[CrossRef](#)]
3. Ponce, S.; Mena-Campoverde, C.; Proaño, J.S.; Álvarez-Barreto, J.F.; Aguirre, F.; Quintana, D.T.; Sanchez Prieto, J.S.; Streitwieser, D.A. Proposal of a regulatory framework for bioenergy implementation in a unified agricultural code for Ecuador. *Biofuels Bioprod. Biorefining* **2022**, *16*, 1116–1129. [[CrossRef](#)]
4. Kumar, H.; Bhardwaj, K.; Sharma, R.; Nepovimova, E.; Kuča, K.; Dhanjal, D.S.; Verma, R.; Bhardwaj, P.; Sharma, S.; Kumar, D. Fruit and Vegetable Peels: Utilization of High Value Horticultural Waste in Novel Industrial Applications. *Molecules* **2020**, *25*, 2812. [[CrossRef](#)]
5. Pathak, P.D.; Mandavgane, S.A.; Kulkarni, B.D. Fruit peel waste: Characterization and its potential uses. *Curr. Sci.* **2017**, *113*, 444–454. [[CrossRef](#)]
6. Mora-Sandí, A.; Ramírez-González, A.; Castillo-Henríquez, L.; Lopretti-Correa, M.; Vega-Baudrit, J.R. Persea Americana Agro-Industrial Waste Biorefinery for Sustainable High-Value-Added Products. *Polymers* **2021**, *13*, 1727. [[CrossRef](#)]
7. Riera, M.A.; Maldonado, S.; Palma, R. Residuos agroindustriales generados en Ecuador para la elaboración de bioplásticos. *Rev. Ing. Ind.* **2019**, *17*, 227–246. [[CrossRef](#)]
8. Dahiya, S.; Kumar, A.N.; Shanthi Srajan, J.; Chatterjee, S.; Sarkar, O.; Mohan, S.V. Food waste biorefinery: Sustainable strategy for circular bioeconomy. *Bioresour. Technol.* **2018**, *248*, 2–12. [[CrossRef](#)]
9. Aboyewa, J.A.; Sibuyi, N.R.S.; Meyer, M.; Oguntibeju, O.O. Green Synthesis of Metallic Nanoparticles Using Some Selected Medicinal Plants from Southern Africa and Their Biological Applications. *Plants* **2021**, *10*, 1929. [[CrossRef](#)]
10. Rafique, M.; Sadaf, I.; Rafique, M.S.; Tahir, M.B. A review on green synthesis of silver nanoparticles and their applications. *Artif. Cells Nanomed. Biotechnol.* **2017**, *45*, 1272–1291. [[CrossRef](#)]
11. Silva, L.P.; Reis, I.G.; Bonatto, C.C. Green Synthesis of Metal Nanoparticles by Plants: Current Trends and Challenges. In *Green Processes for Nanotechnology: From Inorganic to Bioinspired Nanomaterials*; Basiuk, V.A., Basiuk, E.V., Eds.; Springer International Publishing: Cham, Switzerland, 2015; pp. 259–275. ISBN 978-3-319-15461-9.
12. Gherasim, O.; Puiu, R.A.; Bîrcă, A.C.; Burduşel, A.-C.; Grumezescu, A.M. An Updated Review on Silver Nanoparticles in Biomedicine. *Nanomaterials* **2020**, *10*, 2318. [[CrossRef](#)] [[PubMed](#)]
13. Bapat, R.A.; Chaubal, T.V.; Joshi, C.P.; Bapat, P.R.; Choudhury, H.; Pandey, M.; Gorain, B.; Kesharwani, P. An overview of application of silver nanoparticles for biomaterials in dentistry. *Mater. Sci. Eng. C* **2018**, *91*, 881–898. [[CrossRef](#)] [[PubMed](#)]
14. Juarez-Moreno, K.; Gonzalez, E.B.; Girón-Vazquez, N.; Chávez-Santoscoy, R.A.; Mota-Morales, J.D.; Perez-Mozqueda, L.L.; Garcia-Garcia, M.R.; Pestryakov, A.; Bogdanchikova, N. Comparison of cytotoxicity and genotoxicity effects of silver nanoparticles on human cervix and breast cancer cell lines. *Hum. Exp. Toxicol.* **2016**, *36*, 931–948. [[CrossRef](#)] [[PubMed](#)]
15. Narayanamma, A.; Rani, A.; Raju, M.E. Natural synthesis of silver nanoparticles by banana peel extract and as an antibacterial agent. *J. Polym. Text. Eng.* **2016**, *3*, 17–25.
16. Thatikayala, D.; Jayarambabu, N.; Banothu, V.; Ballipalli, C.B.; Park, J.; Rao, K.V. Biogenic synthesis of silver nanoparticles mediated by Theobroma cacao extract: Enhanced antibacterial and photocatalytic activities. *J. Mater. Sci. Mater. Electron.* **2019**, *30*, 17303–17313. [[CrossRef](#)]
17. Girón-Vázquez, N.G.; Gómez-Gutiérrez, C.M.; Soto-Robles, C.A.; Nava, O.; Lugo-Medina, E.; Castrejón-Sánchez, V.H.; Vilchis-Nestor, A.R.; Luque, P.A. Study of the effect of Persea americana seed in the green synthesis of silver nanoparticles and their antimicrobial properties. *Results Phys.* **2019**, *13*, 102142. [[CrossRef](#)]

18. Srikar, S.K.; Giri, D.D.; Pal, D.B.; Mishra, P.K.; Upadhyay, S.N. Light induced green synthesis of silver nanoparticles using aqueous extract of *Prunus amygdalus*. *Green Sustain. Chem.* **2016**, *6*, 26–33. [[CrossRef](#)]
19. Madhu, G.; Kumar, A.S.; Nair, S.K. Sunlight-induced honey-mediated green synthesis of silver nanoparticles. In *AIP Conference Proceedings*; AIP Publishing LLC: Melville, NY, USA, 2019; Volume 2162, p. 20101.
20. Siewert, B.; Stuppner, H. The photoactivity of natural products—An overlooked potential of phytomedicines? *Phytomedicine* **2019**, *60*, 152985. [[CrossRef](#)]
21. Kumar, B.; Angulo, Y.; Smita, K.; Cumbal, L.; Debut, A. Capuli cherry-mediated green synthesis of silver nanoparticles under white solar and blue LED light. *Particuology* **2016**, *24*, 123–128. [[CrossRef](#)]
22. Khlebtsov, B.N.; Khlebtsov, N.G. On the measurement of gold nanoparticle sizes by the dynamic light scattering method. *Colloid J.* **2011**, *73*, 118–127. [[CrossRef](#)]
23. Chouhan, S.; Guleria, S. Green synthesis of AgNPs using *Cannabis sativa* leaf extract: Characterization, antibacterial, anti-yeast and  $\alpha$ -amylase inhibitory activity. *Mater. Sci. Energy Technol.* **2020**, *3*, 536–544. [[CrossRef](#)]
24. Kumar, B.; Smita, K.; Cumbal, L.; Debut, A. Green synthesis of silver nanoparticles using Andean blackberry fruit extract. *Saudi J. Biol. Sci.* **2017**, *24*, 45–50. [[CrossRef](#)] [[PubMed](#)]
25. Singh, P.; Pandit, S.; Garnæs, J.; Tunjic, S.; Mokkaapati, V.R.S.S.; Sultan, A.; Thygesen, A.; Mackevica, A.; Mateiu, R.V.; Daugaard, A.E.; et al. Green synthesis of gold and silver nanoparticles from *Cannabis sativa* (Industrial hemp) and their capacity for biofilm inhibition. *Int. J. Nanomed.* **2018**, *13*, 3571–3591. [[CrossRef](#)] [[PubMed](#)]
26. Kumar, B.; Smita, K.; Cumbal, L.; Camacho, J.; Hernández-gallegos, E.; Chávez-lópez, M.D.G.; Grijalva, M.; Andrade, K. One pot phytosynthesis of gold nanoparticles using *Genipa americana* fruit extract and its biological applications. *Mater. Sci. Eng. C* **2016**, *62*, 725–731. [[CrossRef](#)]
27. Setyawan, H.Y.; Sukardi, S.; Puriwangi, C.A. Phytochemicals properties of avocado seed: A review. *IOP Conf. Ser. Earth Environ. Sci.* **2021**, *733*, 012090. [[CrossRef](#)]
28. Segovia, F.J.; Hidalgo, G.I.; Villasante, J.; Ramis, X.; Almajano, M.P. Avocado seed: A comparative study of antioxidant content and capacity in protecting oil models from oxidation. *Molecules* **2018**, *23*, 2421. [[CrossRef](#)] [[PubMed](#)]
29. Diniardi, E.M.; Argo, B.D.; Wibisono, Y. Antibacterial activity of cocoa pod husk phenolic extract against *Escherichia coli* for food processing. *IOP Conf. Ser. Earth Environ. Sci.* **2020**, *475*, 012006. [[CrossRef](#)]
30. Salayová, A.; Bedlovičová, Z.; Daneu, N.; Baláž, M.; Lukáčová Bujňáková, Z.; Balážová, L.; Tkáčiková, L. Green synthesis of silver nanoparticles with antibacterial activity using various medicinal plant extracts: Morphology and antibacterial efficacy. *Nanomaterials* **2021**, *11*, 1005. [[CrossRef](#)]
31. Jalab, J.; Abdelwahed, W.; Kitaz, A.; Al-Kayali, R. Green synthesis of silver nanoparticles using aqueous extract of *Acacia cyanophylla* and its antibacterial activity. *Heliyon* **2021**, *7*, e08033. [[CrossRef](#)]
32. Lateef, A.; Azeez, M.A.; Asafa, T.B.; Yekeen, T.A.; Akinboro, A.; Oladipo, I.C.; Azeez, L.; Ojo, S.A.; Gueguim-Kana, E.B.; Beukes, L.S. Cocoa pod husk extract-mediated biosynthesis of silver nanoparticles: Its antimicrobial, antioxidant and larvicidal activities. *J. Nanostruct. Chem.* **2016**, *6*, 159–169. [[CrossRef](#)]